

Discovery and Characterization of a Novel Series of Chloropyrimidines as Covalent Inhibitors of the Kinase MSK1

Adrian Hall,* Jan Abendroth, Madison J. Bolejack, Tom Ceska, Sylvie Dell'Aiera, Victoria Ellis, David Fox, III, Cyril François, Muigai M. Muruthi, Camille Prével, Karine Poullennec, Sergei Romanov, Anne Valade, Alain Vanbellinghen, Jason Yano, and Martine Geraerts



Cite This: *ACS Med. Chem. Lett.* 2022, 13, 1099–1108



Read Online

ACCESS |



Metrics & More



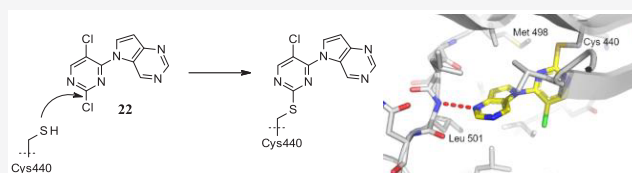
Article Recommendations



Supporting Information

ABSTRACT: We describe the identification and characterization of a series of covalent inhibitors of the C-terminal kinase domain (CTKD) of MSK1. The initial hit was identified via a high-throughput screening and represents a rare example of a covalent inhibitor which acts via an S_NAr reaction of a 2,5-dichloropyrimidine with a cysteine residue (Cys440). The covalent mechanism of action was supported by *in vitro* biochemical experiments and was confirmed by mass spectrometry. Ultimately, the displacement of the 2-chloro moiety was confirmed by crystallization of an inhibitor with the CTKD. We also disclose the crystal structures of three compounds from this series bound to the CTKD of MSK1, in addition to the crystal structures of two unrelated RSK2 covalent inhibitors bound to the CTKD of MSK1.

KEYWORDS: MSK1, RPS6KAS, kinase, covalent inhibitor, chloropyrimidine, cysteine trapping



Covalent inhibitors of kinases have become popular in recent years, with several marketed compounds exerting their activity by this mode. These inhibitors form a covalent bond with a non-catalytic cysteine residue in the orthosteric binding site and, in general, employ a reactive group such as an acrylamide or propynamide which reacts with the cysteine residue.¹ Mapping of the kinome to ascertain which kinases this modality can be applied to has revealed that there are multiple family members with targetable cysteines, which are located in several sub-regions of the ATP binding pocket.^{2–5} While most covalent warheads for non-catalytic cysteines involve reactive functional groups such as α,β -unsaturated amides, there are very few examples of halogenated aromatic heterocycles; however, recent reports on, e.g., HCV NSSA inhibitors from Merck⁶ and FGFR4 inhibitors from Novartis,⁷ are noteworthy. In addition, dichloropyrimidines have been studied as proteome activity probes but were found to be inert, whereas analogous dichlorotriazines were found to react with lysine rather than cysteine.⁸ Interestingly, these dichlorotriazines displayed different reactivity in solution, compared to the proteome, as in solution they prefer cysteine over lysine.

Mitogen- and stress-activated protein kinase 1 (MSK1), also known as ribosomal protein S6 kinase alpha-5 (RPS6KAS), is a nuclear kinase that is activated by upstream kinases such as p38 or ERK.⁹ The RPS6KA family contains six members, MSK1,2 and RSK1–4, all of which are unusual in that they contain two kinase domains: a C-terminal kinase domain (CTKD) and an N-terminal kinase domain (NTKD).¹⁰ The NTKD belongs to the AGC family, while the CTKD belongs to the calcium/calmodulin-dependent protein family. The activation cascade

of MSK1 has been studied in detail. Briefly, phosphorylation by p38 or ERK results in activation of the CTKD which, following autophosphorylation, results in activation of the NTKD, which in turn phosphorylates substrates.^{11,12}

Several substrates of MSK1 have been published, such as CREB and ATF1,¹³ histone H3 and high-mobility-group protein 14 (HMG-14),¹⁴ and Ataxin-1.¹⁵ Due to its substrates and position in the inflammatory kinase cascade, MSK1 has been linked to various diseases,¹⁶ including psoriasis,¹⁷ colorectal cancer,¹⁸ gastric cancer,¹⁹ and spinocerebellar ataxia type 1 (SCA1).¹⁵ Furthermore, it has been implicated in the modulation of IL-17 levels²⁰ and downstream signaling of IL-17,^{21,22} which could associate it with various inflammatory disorders.

Due to the association with various diseases and the paucity of known inhibitors, we initiated a project to identify novel selective inhibitors of MSK1. To date, the best-characterized inhibitor of MSK1 is SB-747651-A,²³ which binds to the NTKD.²⁴ To enable the identification of inhibitors covering multiple modes of action, including orthosteric (at either kinase domain) and allosteric, we set up a biochemical cascade assay. To this end we incubated compounds for 1 h with full-

Received: March 22, 2022

Accepted: June 9, 2022

Published: June 25, 2022



length MSK1 in its inactive form and then activated *in situ* by the addition of ERK2. High-throughput screening (HTS) was conducted in this format (25 μ M ATP) using the Caliper technology to detect phosphorylation of a novel substrate (see Supporting Information for details).²⁵ Initial hits were confirmed via dose–response and cross-screening against ERK2, to remove ERK2 inhibitors. This resulted in numerous hits with different modes of action. A similar screen was conducted for MSK2, and compounds generally showed a similar level of activity at MSK2, as highlighted for selected examples. In this Letter, we describe the identification and characterization of novel 2,5-dichloropyrimidines which we found to act via covalent reaction with Cys440 on the P-loop of the CTKD of MSK1.

The HTS campaign, as described, identified compound **1**, Figure 1. Counter-screening at ERK2 revealed no activity,

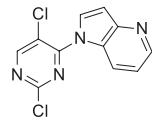
	ERK2-MSK1 cascade pIC ₅₀ 6.7 (1 hr preincubation)
	ERK2-MSK1 cascade pIC ₅₀ 5.6 (no preincubation)
	ERK2-MSK1 cascade pIC ₅₀ 7.2 (3 hr preincubation)
	ERK2-MSK2 cascade pIC ₅₀ 6.1 (1 hr preincubation)
	MSK1 pIC ₅₀ <4
	MSK1 NTKD pIC ₅₀ inactive
	MSK1 CTKD pIC ₅₀ 6.4 / 6.4 (5 μ M / 250 μ M ATP)
	MSK1 CTKD pIC ₅₀ 4.8 / 5.7 (-/+ 1hr preincubation)
	1

Figure 1. Structure of HTS hit **1**, with biochemical data.

demonstrating that the observed activity was due to MSK1 inhibition. Due to its potent activity (pIC₅₀ 6.7, 200 nM), its relatively small nature (MW 265 g/mol), and the presence of the potentially reactive 2,5-dichloropyrimidine, we suspected **1** may be a covalent inhibitor. Initial experiments with a higher ATP concentration (1 mM) showed no shift in potency (pIC₅₀ 6.9), further supporting this hypothesis. Therefore, in order to ascertain the mode of action of **1**, we initiated several parallel activities: synthesis of analogues, detailed pharmacological experiments (including time dependency), mass spectrometry, and structural biology.

At the outset, due to the nature of the cascade assay, we first attempted to elucidate which region of the protein, i.e., the CTKD or NTKD, the compound bound to. In the first instance we tested **1** against the active, full-length MSK1, where only NTKD inhibitors would show activity. In this assay, **1** showed pIC₅₀ < 4 (>100 μ M), strongly supporting that the compound was either an allosteric or a CTKD inhibitor. The lack of activity at the NTKD was later confirmed in a NTKD assay, where the compound showed no activity. Furthermore, in a CTKD assay the compound showed potency that was consistent with data in the initial cascade assay, Figure 1. In the cascade assay, increasing the pre-incubation time with **1** to 3 h before MSK1 activation resulted in a 3-fold increase in potency, whereas no pre-incubation diminished the activity 10-fold (Figure 1), consistent with a covalent mode of action or conformational change of the protein. Subsequent experiments in the CTKD assay with higher ATP concentrations showed no potency shift. Further experiments with the CTKD with no pre-incubation time showed diminished activity. Finally, enzyme activity did not recover following wash out, showing a slow off-rate. Taken together, at this stage of the project, these results were consistent with either a covalent or tight binding interaction.

The hypothesis that the mode of action was covalent was supported by the synthesis of novel analogues which showed the requirement of a 2,5-dihalopyrimidine for activity, and activity decreased sharply without these groups (Table 1).

Table 1. Investigation of the SAR for Replacements of the 2- and 5-Cl Substituents on the Pyrimidine Ring

compd	X	Y	ERK2-MSK1 pIC ₅₀ ^a
1	Cl	Cl	6.7 \pm 0.1 (5)
2	H	Cl	4.9 \pm 0.4 (2)
3	F	Cl	7.7
4	Br	Cl	6.7
5	CN	Cl	5.1
6	Me	Cl	<4.5
7	SMe	Cl	4.75 \pm 0.2 (2)
8	Cl	H	5.8 \pm 0.2 (3)
9	Cl	F	5.9
10	Cl	Me	4.7

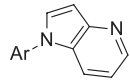
^aData from ERK2-MSK1 cascade assay with 1 h pre-incubation. Data quoted \pm standard deviation (SD) and number of replicates in parentheses when assay performed more than once. Otherwise single value listed.

Deletion of the 2-Cl-atom (X) led to almost 100-fold reduction of activity (**2**). Switching the 2-Cl to F (**3**) increased potency 10-fold, whereas Br (**4**) was equipotent to **1**. Compound **4** also showed similar potency at MSK2 (pIC₅₀ 6.2) to MSK1. Other potentially electrophilic groups such as nitrile (**5**) reduced activity, while Me (**6**) and SMe (**7**) showed minimal or no activity. Note that neither **3** nor **4** showed any potency shift in the presence of a 10-fold higher ATP concentration in the CTKD assay: **3**, pIC₅₀ 6.7 (low and high ATP); **4**, pIC₅₀ 5.7 and 5.8 (low and high ATP). These data are consistent with a potential S_NAr reaction at the 2-position of the pyrimidine and are supported by the higher activity of the 2-fluoro analogue **3**.

Investigation of replacements of the 5-chloro (Y) substituent showed that deletion of the Cl-atom (**8**) resulted in almost 10-fold decrease of activity. The 5-F analogue (**9**) showed similar activity despite the electron-withdrawing nature of the F-atom, which could perhaps be attributed to a conformational effect, i.e., less effect on torsional angle than induced by the Cl-atom in **1**.

The methyl analogue (**10**) showed minimal activity, again highlighting the importance of the Cl substituent. The fluoro derivative (**9**) did not show any shift in potency in the presence of higher ATP concentrations in the CTKD assay (pIC₅₀ 5.0, low and high ATP), again consistent with an uncompetitive/allosteric or covalent mechanism.

We also conducted a broader investigation of 2,5-dichloropyrimidine replacements in order to examine the influence of the reactivity on potency. Data for this area of work are summarized in Table 2. Surprisingly, the pyridine analogue (**11**) was inactive under the same assay conditions, despite its electron-deficient nature, as were the dichlorophenyl analogue (**12**) and the chloropyridine (**13**), implying that both N-atoms of the pyrimidine are required. Interestingly, the isomeric

Table 2. Investigation of the SAR for Replacements of the 5-Dichloropyrimidin-4-yl Ring


Cmpd	Ar	^a ERK2-MSK1 pIC ₅₀
1		6.7 ± 0.1 (5)
11		<4.5
12		<4.5
13		<4.5
14		7.1
15		6.5
16		6.7
17		4.5
18		4.7

^aData from ERK2-MSK1 cascade assay with 1 h pre-incubation. Data quoted ± standard deviation (SD) and number of replicates in parentheses when assay performed more than once. Otherwise single value listed.

monochloropyrimidine (**14**) displayed slightly enhanced activity compared to **1**, highlighting that the pyrimidine is required for sufficient electrophilicity. Compound **14** did not show a potency shift in the presence of higher ATP concentrations in the CTKD assay, pIC₅₀ 6.1 (low and high ATP), suggesting that the mechanism of action was unchanged. Substitution *ortho* to the Cl-atom of **14**, such as **15** or **16**, resulted in a slight reduction of potency, regardless of the nature of the group, probably due to steric hindrance of the reactive site. Again, **16** showed similar activity at MSK2 (pIC₅₀ 6.4). Finally, the un-halogenated pyrimidines **17** and **18** showed only residual activity.

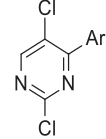
Shifting attention to the 4-azaindole of **1**, alternatives were sought on the premise that this group may be interacting with the hinge region of the CTKD. Shifting the indole N-1 to provide an HBD, as in azaindole **19** provided little gain, implying that the potential HBD available on the azaindole was not optimally positioned or there was a substantial energy penalty, for example desolvation. Compound **19** showed slightly weaker activity at MSK2 (pIC₅₀ 6.2). Switching to both N- and C-linked pyrrolopyrimidines, **20** and **21**, respectively, resulted in an almost 10-fold boost in potency over **1**. The fact that **21** was equipotent to **20** again supports

the lack of HBD interaction, in a similar manner to **1** versus **19**.

In line with other compounds, **20** did not show a decrease in activity with higher ATP in the CTKD assay, pIC₅₀ 7.2 (low and high ATP).

Both **20** (ER2-MSK2 pIC₅₀ 7.0) and **21** (ERK2-MSK2 pIC₅₀ 7.1) showed similar levels of activity at MSK2.

As the isomeric monochloropyrimidine derivative **14** (Table 2) had shown better potency than **1**, we prepared analogues of **14** where the 4-azaindole was replaced with groups identified in Table 3. The results revealed a similar boost in potency to

Table 3. Investigation of the SAR for Replacements of the 4-Azaindole


Cmpd	Ar	^a ERK2-MSK1 pIC ₅₀
1		6.7 ± 0.1 (5)
19		7.0 ± 0.4 (3)
20		7.5 ± 0.3 (2)
21		7.7 ± 0.1 (4)

^aData from ERK2-MSK1 cascade assay with 1 h pre-incubation. Data quoted ± standard deviation (SD) and number of replicates in parentheses when assay performed more than once. Otherwise single value listed.

that when comparing **1** to **20**, and led to the identification of **22** which also demonstrated an almost 10-fold increase in potency relative to **14** (Figure 2).

Finally, despite the fact that replacement of the chloropyrimidine by chloropyridines, such as **11** and **13** (Table 2), resulted in complete loss of activity, we were interested to see if activity could be regained with the newly identified pyrrolopyrimidine. In addition, we also changed the electron-withdrawing group on the pyridine and investigated both *para*- and *ortho*-positions relative to the presumed S_NAr site. Thus, compounds **23** and **24** were prepared (Figure 2). Surprisingly, *para*-cyano derivative **23** displayed activity equivalent to that of **22** and was 3-fold more potent than the chloropyrimidine analogue **20**; however, the activity was reduced by 10-fold when the nitrile moiety was shifted *ortho* to the Cl-atom (**24**).

In order to further characterize the mode of action, several compounds were selected for more detailed biochemical characterization, i.e., jump dilution experiments. Compounds were pre-incubated with inactive MSK1 at ~20 × IC₅₀ for 3 h without ATP, after which the complex was diluted into a buffer solution containing 25 mM ATP and 0.5 mM peptide substrate. Kinetic analysis of substrate–product formation was conducted for around 7 h. As can be seen in Table 4, enzyme activity was fully recovered with a control (non-covalent analogue) compound,²⁸ whereas compounds **14**, **19**,

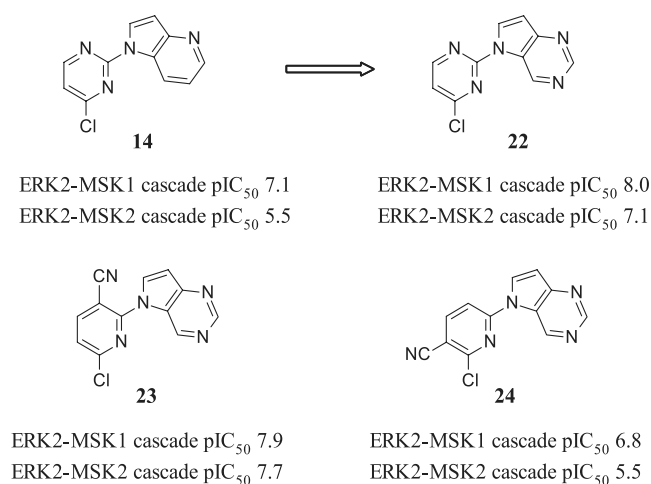


Figure 2. Replacement of the azaindole in **14** by the pyrrolopyrimidine in **22** results in an almost 10-fold increase in potency. Chloropyrimidine **23** shows that it is possible to achieve high potency with aromatic heterocycles other than pyrimidine, while the isomeric derivative **24** is approximately 10-fold less active.

Table 4. Residence Time Analysis in ERK2-MSK1 Biochemical Assay by Jump Dilution

compd	K_{obs} (s ⁻¹)	V_s	max recovery (% control)	estimated residence time (min)
control ²⁸	1.75×10^{-4}	4.57×10^{-3}	96	8–14
14	6.65×10^{-6}	3.08×10^{-4}	6	1488–1675
19	8.28×10^{-6}	3.84×10^{-4}	8	1332–1552
20	7.62×10^{-6}	5.09×10^{-4}	11	1457–1561
DMSO	1.98×10^{-4}	4.76×10^{-3}		

and **20** showed around 10% recovery of activity, which resulted in a long residence time, adding further support to a covalent mode of inhibition. Taken together, the data in Tables 1–4 and Figure 2 are strongly supportive of a covalent mode of action.

In parallel to the SAR investigations, we also conducted mass spectrometry experiments, where the CTKD was incubated with various compounds. Data from these experiments are summarized in Table 5. In addition to the compounds described herein, we also included two literature compounds that have been characterized as reversible covalent inhibitors of the RPS6KA3 (RSK2) kinase, namely **25** and **26** (Figure 3). Compound **25** was described as a reversible covalent inhibitor of RSK2, whereby the Michael acceptor forms a covalent bond with Cys436 in the CTKD of RSK2.²⁶ This compound was also described to inhibit MSK1,2 and RSK3 and was therefore studied. In addition, compound **26** has also been described as a reversible covalent inhibitor of RSK2 and confirmed to have a similar mode of action.²⁷

As mentioned previously, RSK2 is a closely related kinase and has a similarly positioned cysteine to MSK1, and **25** is known to cross react with MSK1. Thus, we profiled both compounds in our biochemical cascade assay, where they showed strong activity (Figure 3). Furthermore, the activity of **26** was confirmed to be via inhibition of the CTKD, via biochemical assay (Figure 3). Subsequently, we successfully solved the structures of both compounds with the CTKD of MSK1, *vide infra*.

Table 5. Summary of Native Mass Spectrometry and LCMS Experiments with MSK1 CTKD

compd	native mass spec	LCMS
1	1 min: 29% (1:1) 1 h: 100% (1:1)	1 min: 22% (1:1) 1 h: 81% (1:1) 24 h: 57% (1:1), 31% (1:2), 11% (1:3)
14	1 min: 9% (1:1) 1 h: 92% (1:1) 3 h: 100% (1:1)	1 min: 0% 1 h: 22% (1:1) 3 h: 47% (1:1) 24 h: 94% (1:1)
22	1 min: 47% (1:1) 1 h: 100% (1:1) 3 h: 100% (1:1)	1 min: 0% 1 h: 97% (1:1) 3 h: 92% (1:1) 24 h: 100% (1:1)
25	1 min: 54% (1:1) 1 h: 63% (1:1)	1 min: 16% (1:1) 1 h: 10% (1:1) 24 h: 15% (1:1)
26	1 min: 93% (1:1), 7% (1:2) 1 h: 81% (1:1), 16% (1:2), 2% (1:3)	1 min: 50% (1:1), 32% (1:2), 6% (1:3) 1 h: 6% (1:1), 43% (1:2), 32% (1:3), 11% (1:4) 24 h: 24% (1:1), 34% (1:2), 26% (1:3), 10% (1:4)

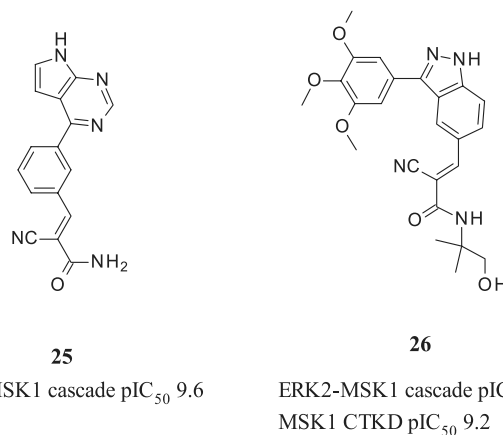


Figure 3. Structures and biochemical data for RSK2 inhibitors **25** and **26**.

To assess if compounds were covalent inhibitors, MSK1 CTKD (10 μM) was incubated at various times with compounds (100 μM) and assessed by native mass spectrometry (binding) and LCMS (covalent binding). Data from these experiments is summarized in Table 5.

The LCMS data in Table 5 confirm that all compounds tested covalently modify MSK1 CTKD. For compounds **1**, **14**, and **22**, the native mass spectrometry data imply all protein was bound with compounds after 1 h incubation with 1:1 stoichiometry. Similarly, the LCMS data for **1** show near-complete adduct formation after 1 h, but after 24 h there appears to be additional labeling, implying a lack of specificity. Compound **14** appears to form the covalent adduct more slowly but with higher specificity, whereas compound **22** appears to both react faster and maintain specificity. Thus, the isomeric monochloropyrimidine present in **14** and **22** appears

to dampen the reactivity compared to the dichloropyrimidine in **1**, thus increasing specificity, while the pyrrolopyrimidine can increase reaction rate over the 4-azaindole, **22** versus **14**. Interestingly, with MSK1 compound **25** appears to bind well, but not all of this binding is covalent, or the covalent bond formation is reversible under the LCMS experimental conditions, as the covalent adduct measured is less than 20%. For compound **26**, the data suggest that multiple covalent adducts are formed, implying a lack of specificity.

Furthermore, mass spectrometry data showed a MW increase of 227 Da for **1**, 194 Da for **14**, 195 Da for **22**, 289 Da for **25**, and 450 Da for **26**. Taken together, these results are consistent with the Michael addition to compounds **25** and **26**, and the S_NAr reaction with loss of Cl to compounds **1** (loss of Cl in the 2-position of the pyrimidine), **14**, and **22**, as depicted in Figure 4 for **1** and **23**.

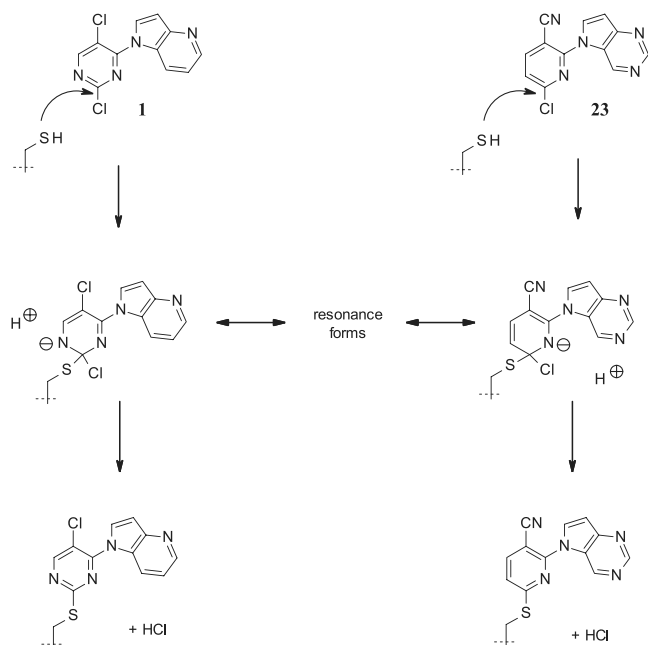


Figure 4. Proposed reactions of compounds **1** and **23** with Cys440 of MSK1 CTKD.

A subsequent experiment with **1** with 1 h incubation followed by tryptic digestion confirmed the covalent attachment to Cys440 (see Supporting Information).

At the time of this work, there were only two crystal structures of the CTKD in the public domain, one apo (PDB: 3KN6) and one with AMP-PNP (PDB: 3KNS), which had not changed at the timing of writing.

In order to better understand how the compounds bound to MSK1 CTKD, several compounds were selected for crystallography. From these experiments we obtained three crystal structures with novel compounds described herein, all of which confirmed covalent bond formation with Cys440 and the anticipated interaction with the hinge region.

Structures were obtained with **20**, its 5-bromo-2-chloropyrimidine analogue (**27**, pI_{C50} 7.5), and the 6-chloro-3-cyanopyrimidine derivative **23** (Figures 5 and 6).

The structure of the CTKD with **20** (Figure 5a, PDB: 7UP4) confirms that the compound binds to the ATP site and interacts with the hinge region, with the N-atom of the pyrrolopyrimidine accepting a H-bond from Leu501. The

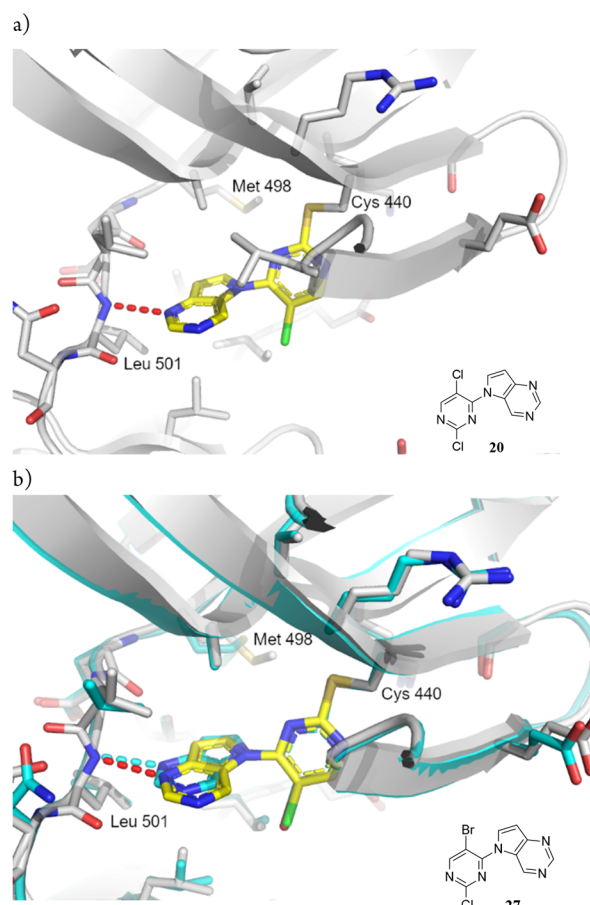


Figure 5. (a) Crystal structure of **20** and the CTKD (PDB: 7UP4), showing a type I binding mode with a hydrogen-bond-accepting (HBA) interaction with NH of Leu501. Covalent interaction with Cys440 is shown, replacing the chlorine atom attached to the carbon between the pyrimidine nitrogen atoms. (b) Overlay of the crystal structures of **20** and **27**, showing the same binding mode and interactions, namely a HBA interaction with NH of Leu501. Covalent interaction with Cys440 is shown.

chloropyrimidine is approximately 60° out of plane of the pyrrolopyrimidine, likely facilitated by the 5-Cl-atom, which positions the ring to allow reaction with Cys440 and form a covalent adduct as seen in Figure 5a, confirming our hypothesis. There appear to be opportunities to push out from the pyrrolopyrimidine toward the gatekeeper Met498, which may help in designing both affinity and selectivity.

We also obtained a crystal structure with the bromo analogue of compound **20**, i.e., compound **27** (equipotent, Figure 5b, PDB: 7UP8), which showed a similar binding mode, as can be seen in Figure 5b, with the overlay of both structures.

The third crystal structure, with **23** (PDB: 7UP5), revealed a similar interaction between the pyrrolopyrimidine moiety and the hinge region but an unexpected rotation of the cyanopyrimidine ring (Figure 6a). This juxtaposition also positions the nitrile group toward the DFG motif, where it potentially makes a weak H-bond with the backbone of Asp565.²⁹

The differences in the binding modes of **20** and **23** are depicted in Figure 6b, which shows an overlay of both compounds. Thus, although the electron-deficient aromatic heterocycles occupy different regions of the pocket, the twist in both results in the reactive site overlapping in both structures and facilitates reaction with Cys440. Therefore, only a minor

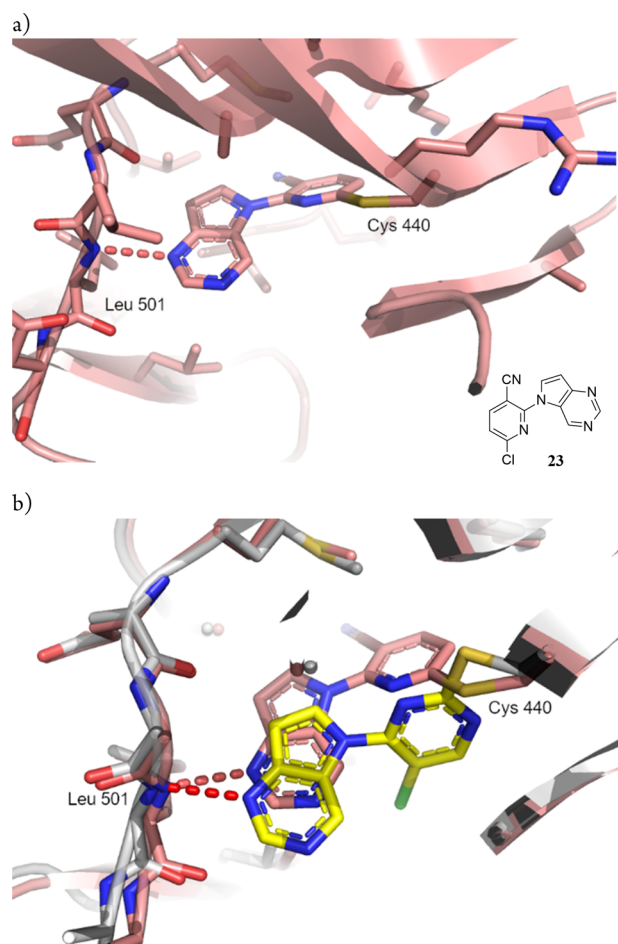


Figure 6. (a) Crystal structure of **23** (PDB: 7UP5), showing that the pyrrolopyrimidine N-atom still accepts a H-bond from the NH of Leu501. Covalent interaction with Cys440 is shown. (b) Overlay of the crystal structures of **20** and **23**, highlighting the different binding modes and the different positions of the covalent traps. The reactive C-atom is in a similar location, but the aromatic rings are orthogonal to one another.

rotation of 26° of the Cys 440 side chain is required to accommodate each of the two compounds **20** and **23**. The nitrile on the pyridine of **23** accepting a H-bond from the backbone of Asp585 likely results in the “flipped” conformation of the pyridyl moiety compared to the pyrimidine in **20**.

In addition to the structural biology with the inhibitors from this series, we successfully solved the structures of both compounds **25** and **26** with the CTKD of MSK1 (Figures 7 and 8).

The structure of **25** with MSK1 CTKD is depicted in Figure 7a (PDB: 7UP6) and shows a bidentate interaction between the pyrrolopyrimidine and the hinge region. The NH donates a H-bond to the carbonyl of Glu499, and the N-atom accepts a H-bond from the backbone NH of Leu501. In addition, the C–H of the pyrimidine potentially forms a weak interaction with the carbonyl of Leu501. The reactive Michael acceptor is in a location similar to the reactive center of **23**, although the side chain of Cys440 approaches from a different angle.

Additional interactions between the protein and the ligand are formed via the amide carbonyl with the hydroxyl of Ser438. The NH₂ of the amide interacts with the carboxylate of Asp565 and forms a water-mediated H-bond with the side chain of

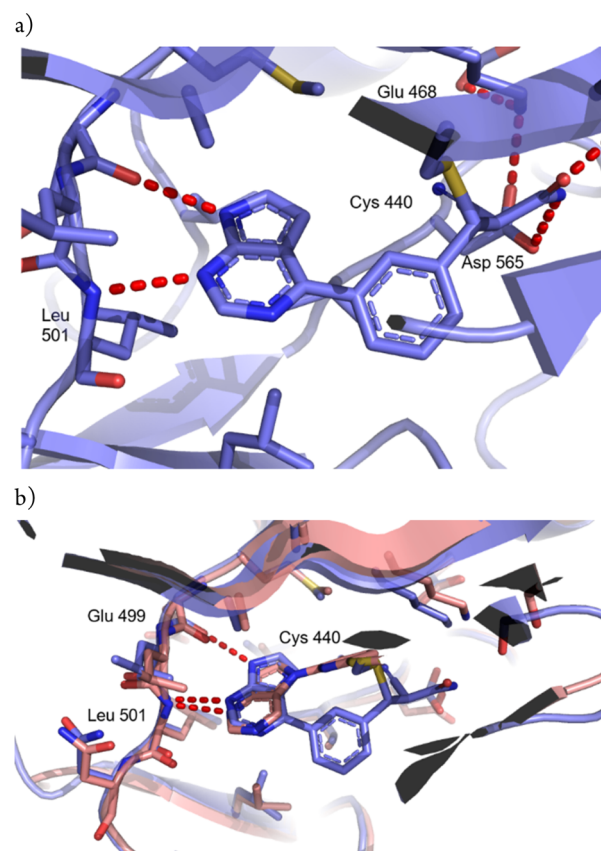


Figure 7. (a) Structure of **25** with the CTKD of MSK1 (PDB: 7UP6) showing covalent bond formation with Cys440. (b) Overlay of the structures of **25** and **23**, highlighting the similar positioning of the pyrrolopyrimidine.

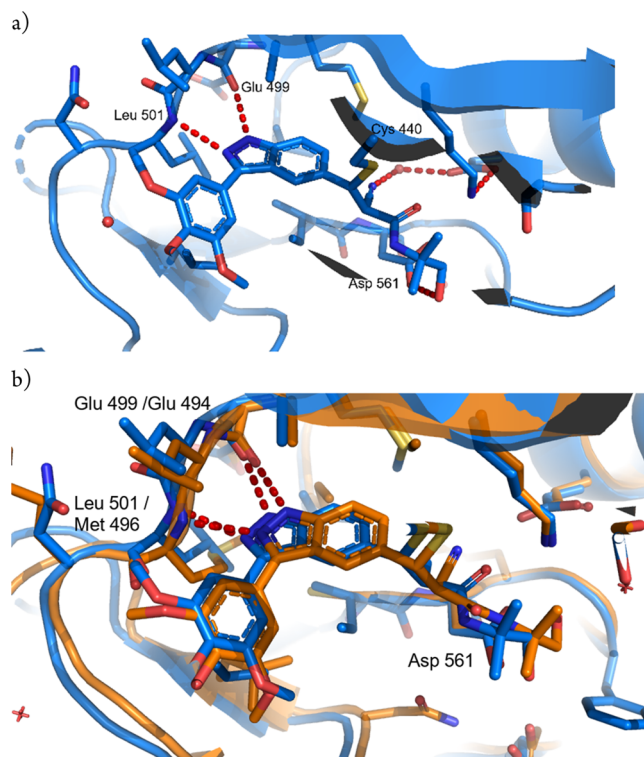


Figure 8. (a) Structure of **26** with the CTKD of MSK1 (PDB: 7UP7). (b) Overlay of the structures of **26** in MSK1 and RSK2 (PDB: 4JGB).

Asn549, and the nitrile forms a water-mediated H-bond with the side chain of Asp565.

An overlay of **23** and **25** is shown in Figure 7b and depicts the similarities and differences in binding modes. This also highlights that it may be possible to target the covalent interaction with Cys440 by making analogues of **23** where a phenyl ring with a cysteine trap is placed in the 7-position of the pyrrolopyrimidine, rather than the 1-position.

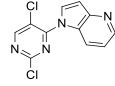
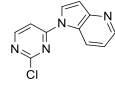
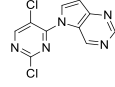
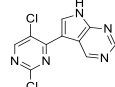
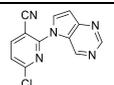
The structure of **26** with the MSK1 CTKD is depicted in Figure 8a (PDB: 7UP7) and shows that the ligand is considerably displaced relative to the other structures, due to the alternative hinge binding motif. The ligand makes several interactions with the protein, including a hydrogen-bond-accepting (HBA) interaction with Leu501 and a hydrogen-bond-donating (HBD) interaction with Glu499. An additional suboptimal H-bond can be seen between the terminal hydroxyl group on the amide moiety and Asp561, while the nitrile moiety of **26** potentially interacts directly with the NH of Asp565 in addition to forming a water-mediated H-bond with the backbone nitrogen of Glu468.

Overall, the structure of **26** with MSK1 is similar to that with RSK2 (PDB: 4JG8, Figure 8b). The polar interactions of **26** with the carbonyl group of Glu 499 (Glu 494 in RSK2) and the backbone nitrogen of Leu 501 (Met 496 in RSK2) are conserved, as is the overall protein environment. The interactions with Asp561 are not conserved between the two structures, which is likely due to different interpretations of the electron density in the two structures.

In addition to the SAR against MSK1, further characterization studies were performed on selected compounds which highlighted several issues, including low solubility and poor *in vitro* metabolic stability. For example, for compound **1**, logD = 2.3, MLM $CL_{int} = 131 \mu\text{L}/\text{min}/\text{mg}$ protein, and HLM $CL_{int} = 11.7 \mu\text{L}/\text{min}/\text{mg}$ protein. Furthermore, GSH trapping experiments were conducted in the presence and absence of metabolic activation (HLM), as we were concerned about the inherent reactivity of compounds from this series. Although minimal GSH adduct formation was detected in the absence of metabolic activation (3% for **1**), extensive glutathione adduct formation was detected with metabolic activation (96% for **1**) (Table 6). Assessment of additional compounds in GSH experiments showed low levels of GSH incorporation in the absence of metabolic activation (Table 6). The low levels of GSH adduct formation in solution could be interpreted as the compounds having low levels of reactivity. However, the mass spectrometry experiments (LCMS, Table 5) show that, in the protein environment, compounds react rapidly, e.g., **1**, which showed reactivity after 1 min and extensive adduct formation after 1 h, and which appears to form multiple adducts after 24 h (on the basis of the stoichiometry). Therefore, the use of solution GSH results to predict proteome cysteine reactivity should be done with caution.

Unfortunately, structural modifications that reduced inherent reactivity also reduced biochemical inhibition, thus implying that the activity was largely driven by the covalent bond formation. Furthermore, the S_NAr mechanism would result in irreversible inhibition, thus resulting in a protein adduct even upon unfolding or degradation, which raised concerns about immunological reactivity. As a result of these data, we shifted our focus to alternative series. However, the results outlined herein may be useful to other research groups who identify electron-deficient aromatic heterocycles as hits. It is also of interest that the compounds are clearly reactive in

Table 6. Summary of GSH Incorporation Experiments in the Absence (–) and Presence (+) of Human Liver Microsomes (HLM)^a

Cmpd	Structure	%GSH – HLM	% GSH + HLM
1		3.0%	96.0%
8		0.1%	53.5%
20		2.5%	99.9%
21		0%	16.1%
23		2.8%	49.9%

^aCompounds (10 μM) incubated with GSH (5 mM) at 37 °C for 30 min in the absence or presence of HLMs.

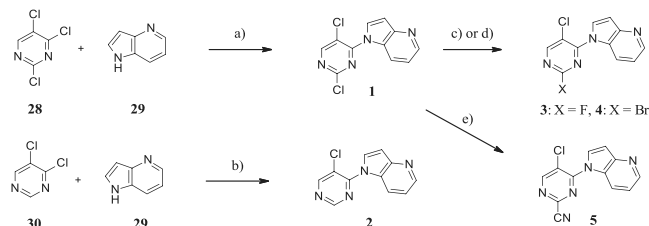
complex with the protein but are relatively resistant to reaction with sulfur nucleophiles such as glutathione in the absence of metabolic activation. If a reactivity screen of this type was used to filter electrophilic compounds, the underlying mechanism of action may be missed.

To assess kinome selectivity, compounds **1** and **23** were profiled in a kinase diversity panel (65 targets, see Supporting Information), where they showed little inhibition of any of the tested targets up to 10 μM . This panel included RSK1,2 and PLK3, which have cysteines at a similar position to MSK1 CTKD,⁵ therefore demonstrating that specificity for MSK1 is achievable. In addition, compounds **21** and **22** were profiled in a panel of 468 kinases³⁰ at a concentration of 10 μM (see Supporting Information). This panel includes all 11 kinases with a Cys at a similar position (MAP3K1, PLK1,2,3, RIPK5, RSK1,2,3,4, and MSK1,2 CTKD).⁵ Of these, other than MSK1,2, only PLK2 and RSK1 were inhibited, thus demonstrating that this series of compounds can achieve selectivity even over kinases that have a similarly positioned cysteine. The fact that RSK1 was not inhibited by **1** or **23** is likely due to assay differences and serves as a note of caution when interpreting selectivity data. In terms of overall kinome selectivity, **22** shows a much better profile than **21**; S35 = 0.03 and S10 = 0.005 for **22** versus S35 = 0.146 and S10 = 0.045 for **21**, likely due to the hinge binding motif, rather than the higher reactivity of the dichloropyrimidine present in **21**, based on the selectivity over the 11 kinases with a cysteine in the same location. For **22**, the targets inhibited at >65% were AAK1 (77%), FLT3 (74%), HASPIN (75%), MAP4K2 (69%), MEK5 (78%), PI3KCB (79%), PLK2 (82%), RIPK4 (69%), RSK1 (73%), VRK2 (85%), and YSK4 (96%), in addition to MSK1 (86%) and MSK2 (96%). Thus, compounds such as **21** demonstrate that kinome selectivity is feasible, even over

kinases with a similarly positioned cysteine, and highlight the potential of these chloro-aromatic heterocyclic derivatives as covalent probes.

Compounds were prepared as outlined in Schemes 1 and 2.^{31,32} Briefly, reaction of the requisite Cl-substituted aromatic heterocycle, e.g., **28**, with an azaindole derivative, e.g., **29**, in the presence of a base, such as NaH, exemplified by compound **1**, or K₂CO₃, exemplified by compound **2**, delivered the desired compounds. Compound **1** could be transformed into analogues such as **3**, **4**, and **5** as outlined in Scheme 1.

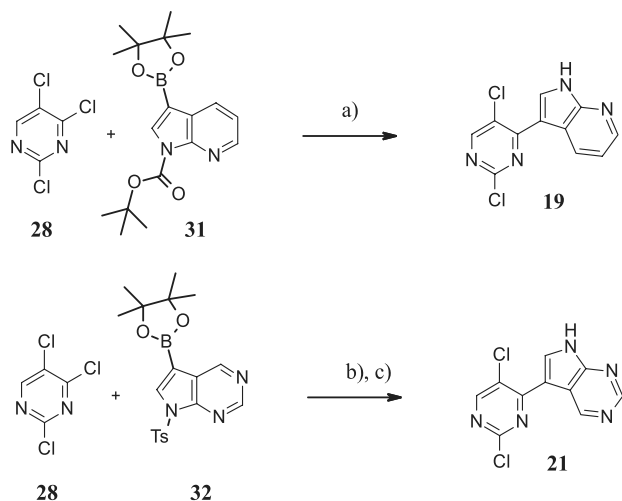
Scheme 1. Representative Syntheses of N-Substituted Azaindoles^a



^aReagents and conditions: (a) NaH, DMF, rt, 33%. (b) K₂CO₃, DMF, rt, 55%. (c) KF, MeCN, 18-crown-6, 40 °C, 29%. (d) AcOH, HBr, 80 °C, 3%. (e) KCN, DABCO, DMSO–H₂O (3:1), 60 °C, 15%.

C-linked derivatives **19** and **21** were prepared as described in Scheme 2. A palladium-mediated coupling of trichloropyrimidine **28** with **31** directly yielded **19**. Tosyl derivative **32** underwent reaction with **28** to give the tosyl-protected intermediate, which provided **21** upon hydrolysis of the tosyl group.

Scheme 2. Representative Syntheses of C-Substituted Azaindole and Pyrrolopyrimidine^a



^aReagents and conditions: (a) Na₂CO₃, Pd(dppf)Cl₂, H₂O, dioxane, 80 °C, microwave, 7%. (b) Na₂CO₃, Pd(PPh₃)₄, H₂O, dioxane, 80 °C, microwave, 42%. (c) DCM, 1 M TBAF in THF, rt, 44%.

In summary, we have detailed the identification of a novel chloropyrimidine/chlorocyanopyridine series of inhibitors of MSK1 CTKD, which act via covalent labeling of Cys440. This adds to the scant literature focused on covalent inhibitors acting via an S_NAr reaction with a non-catalytic cysteine. This

information and characterizing data should be of broad utility to those involved in drug discovery.

■ ASSOCIATED CONTENT

Supporting Information

The Supporting Information is available free of charge at <https://pubs.acs.org/doi/10.1021/acsmmedchemlett.2c00134>.

Synthetic procedures, assay details, mass spectrometry and covalent binding study protocols, GSH assay protocol, kinase selectivity data, discussion on Cys440 reactivity, and literature data on the half-life of MSK1 and related kinases (PDF)

Accession Codes

The five new crystal structures reported herein have been deposited in the Protein Data Bank (PDB), with codes denoted in the discussion. The full list is included here for clarity (all with the CTKD of MSK1): 7UP4 (compound **20**), 7UP5 (compound **23**), 7UP6 (compound **25**), 7UP7 (compound **26**), and 7UP8 (compound **27**).

■ AUTHOR INFORMATION

Corresponding Author

Adrian Hall – UCB, Braine-L'Alleud 1420, Belgium;

orcid.org/0000-0001-7869-6835; Email: adrian.hall@ucb.com

Authors

Jan Ambroth – UCB Seattle, Bainbridge Island, Washington 98110, United States

Madison J. Bolejack – UCB Seattle, Bainbridge Island, Washington 98110, United States; orcid.org/0000-0002-0911-2338

Tom Ceska – UCB, Slough SL1 3WE, U.K.

Sylvie Dell'Aiera – UCB, Braine-L'Alleud 1420, Belgium

Victoria Ellis – UCB, Slough SL1 3WE, U.K.

David Fox, III – UCB Seattle, Bainbridge Island, Washington 98110, United States

Cyril François – NovAliX, Braine-L'Alleud 1420, Belgium

Muigai M. Muruthi – UCB Seattle, Bainbridge Island, Washington 98110, United States

Camille Prével – UCB, Braine-L'Alleud 1420, Belgium

Karine Poullennec – UCB, Braine-L'Alleud 1420, Belgium

Sergei Romanov – NANOSYN, Santa Clara, California 95051, United States

Anne Valade – UCB, Braine-L'Alleud 1420, Belgium

Alain Vanbellinghen – UCB, Braine-L'Alleud 1420, Belgium

Jason Yano – UCB Boston, Cambridge, Massachusetts 02140, United States; Present Address: LifeMine Therapeutics, Cambridge Discovery Park, 30 Acorn Park Dr., Cambridge, MA 02140, USA

Martine Geraerts – UCB, Braine-L'Alleud 1420, Belgium

Complete contact information is available at:

<https://pubs.acs.org/doi/10.1021/acsmmedchemlett.2c00134>

Funding

The work was funded by UCB.

Notes

The authors declare the following competing financial interest(s): Some of the authors may hold stock, stock awards, or stock options in the companies which employ them.

ACKNOWLEDGMENTS

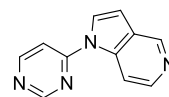
We thank Laurent Calmus (NovAlis) for the synthesis of compound 1. We would also like to thank the following scientists who contributed to the cloning, expression, and purification of MSK proteins: Jessica Williamson, Ellen Wallace, Rena Grice, Ruth Baydo, Jean Lamisere, Victoria Hull, Sujatha Nagulapalli, Doug Austen, Junru Wang, Renée LeBlanc, Sagarika Utture, Terry Webb, Jameson Bullen, and Matt Stigliano.

ABBREVIATIONS

AcOH, acetic acid; DCM, dichloromethane; DABCO, 1,4-diazabicyclo[2.2.2]octane; DMF, dimethylformamide; DMSO, dimethyl sulfoxide; GSH, glutathione; MeCN, acetonitrile; HLM, human liver microsome; MLM, mouse liver microsome; MSK, mitogen and stress-activated protein kinase; CTKD, C-terminal kinase domain; NTKD, N-terminal kinase domain; RSK, ribosomal S6 kinase; TBAF, tetrabutylammonium fluoride; THF, tetrahydrofuran

REFERENCES

- (1) Roskoski, R., Jr. Orally Effective FDA-Approved Protein Kinase Targeted Covalent Inhibitors (TCIs). *Pharm. Res.* **2021**, *165*, 105422.
- (2) Gehring, M. Covalent Kinase Inhibitors: An Overview. *Top. Med. Chem.* **2020**, *36*, 43–94.
- (3) Zhao, Z.; Liu, Q.; Bliven, S.; Xie, L.; Bourne, P. E. Determining Cysteines Available for Covalent Inhibition Across the Human Kinome. *J. Med. Chem.* **2017**, *60*, 2879–2889.
- (4) Chaikuad, A.; Koch, P.; Laufer, S. A.; Knapp, S. The Cysteineome of Protein Kinases as a Target in Drug Development. *Angew. Chem., Int. Ed.* **2018**, *57*, 4372–4385.
- (5) Liu, Q.; Sabnis, Y.; Zhao, Z.; Zhang, T.; Buhrlage, S. J.; Jones, L. H.; Gray, N. S. Developing Irreversible Inhibitors of the Protein Kinase Cysteineome. *Chem. Biol.* **2013**, *20*, 146–159.
- (6) Zeng, Q.; Nair, A. G.; Rosenblum, S. B.; Huang, H.-C.; Lesburg, C. A.; Jiang, Y.; Selyutin, O.; Chan, T.-Y.; Bennett, F.; Chen, K. X.; Venkatraman, S.; Sannigrahi, M.; Velazquez, F.; Duca, J. S.; Gavalas, S.; Huang, Y.; Pu, H.; Wang, L.; Pinto, P.; Vibulbhan, B.; Agrawal, S.; Ferrari, E.; Jiang, C.-K.; Li, C.; Hesk, D.; Gesell, J.; Sorota, S.; Shih, N.-Y.; Njoroge, F. G.; Kozlowski, J. A. Discovery of an Irreversible HCV NS5B Polymerase Inhibitor. *Bioorg. Med. Chem. Lett.* **2013**, *23*, 6585–6587.
- (7) Fairhurst, R. A.; Knoepfel, T.; Leblanc, C.; Buschmann, N.; Gaul, C.; Blank, J.; Galuba, I.; Trappe, J.; Zou, C.; Voshol, J.; Genick, C.; Brunet-Lefevre, P.; Bitsch, F.; Graus-Porta, D.; Furet, P. Approaches to Selective Fibroblast Growth Factor Receptor 4 Inhibition Through Targeting the ATP-Pocket Middle-Hinge Region. *Med. Chem. Commun.* **2017**, *8*, 1604–1613.
- (8) Shannon, D. A.; Banerjee, R.; Webster, E. R.; Bak, D. W.; Wang, C.; Weerapana, E. Investigating the Proteome Reactivity and Selectivity of Aryl Halides. *J. Am. Chem. Soc.* **2014**, *136*, 3330–3333.
- (9) Deak, M.; Clifton, A. D.; Lucocq, J. M.; Alessi, D. R. Mitogen- and Stress-Activated Protein Kinase-1 (MSK1) is Directly Activated by MAPK and SAPK2/p38, and May Mediate Activation of CREB. *EMBO J.* **1998**, *17*, 4426–4441.
- (10) Pearce, L. R.; Komander, D.; Alessi, D. R. The Nuts and Bolts of AGC Protein Kinases. *Nat. Mol. Cell Biol.* **2010**, *11*, 9–22.
- (11) McCoy, C. E.; Campbell, D. G.; Deak, M.; Bloomberg, G. B.; Arthur, J. S. C. MSK1 Activity is Controlled by Multiple Phosphorylation Sites. *Biochem. J.* **2005**, *387*, 507–517.
- (12) McCoy, C. E.; Macdonald, A.; Morrice, N. A.; Campbell, D. G.; Deak, M.; Toth, R.; McIlrath, J.; Arthur, J. S. C. Identification of Novel Phosphorylation Sites in MSK1 by Precursor Ion Scanning MS. *Biochem. J.* **2007**, *402*, 491–501.
- (13) Wiggin, G. R.; Soloaga, A.; Foster, J. M.; Murray-Tait, V.; Cohen, P.; Arthur, J. S. C. MSK1 and MSK1 Are Required for the Mitogen- and Stress-Induced Phosphorylation of CREB and ATF1 in Fibroblasts. *Mol. Cell Biol.* **2002**, *22*, 2871–2881.
- (14) Soloaga, A.; Thomson, S.; Wiggin, G. R.; Rampersaud, N.; Dyson, M. H.; Hazzalin, C. A.; Mahadevan, L. C.; Arthur, J. S. C. MSK2 and MSK1 Mediate the Mitogen- and Stress-Induced Phosphorylation of Histone H3 and HMG-14. *EMBO J.* **2003**, *22*, 2788–2797.
- (15) Park, J.; Al-Ramahi, I.; Tan, Q.; Mollema, N.; Diaz-Garcia, J. R.; Gallego-Flores, T.; Lu, H.-C.; Lagalwar, S.; Duvick, L.; Kang, H.; Lee, Y.; Jafar-Nejad, P.; Sayegh, L. S.; Richman, R.; Liu, X.; Gao, Y.; Shaw, C. A.; Arthur, J. S. C.; Orr, H. T.; Westbrook, T. F.; Botas, J.; Zoghbi, H. Y. RAS-MAPK-MSK1 Pathway Modulates Ataxin1 Protein Levels and Toxicity in SCA1. *Nature* **2013**, *498*, 325–331.
- (16) Reyskens, K. M. S. E.; Arthur, J. S. C. Emerging Roles of the Mitogen and Stress Activated Kinases MSK1 and MSK2. *Front. Cell Dev. Biol.* **2016**, *4*, 56.
- (17) Funding, A. T.; Johansen, C.; Kragballe, K.; Otkjaer, K.; Jensen, U. B.; Madsen, M. W.; Fjording, M. S.; Finnemann, J.; Skak-Nielsen, T.; Paludan, S.; Iversen, L. Mitogen- and Stress-Activated Protein Kinase 1 Is Activated in Lesional Psoriatic Epidermis and Regulates the Expression of Pro-Inflammatory Cytokines. *J. Investigative Dermatol.* **2006**, *126*, 1784–1791.
- (18) Fu, X.; Fan, X.; Hu, J.; Zou, H.; Chen, Z.; Liu, Q.; Ni, B.; Tan, X.; Su, Q.; Wang, J.; Wang, L.; Wang, J. Overexpression of MSK1 is Associated with Tumor Aggressiveness and Poor Prognosis in Colorectal Cancer. *Digestive Liver Disease* **2017**, *49*, 683–691.
- (19) Khan, S. A.; Amnekar, R.; Khade, B.; Barreto, S. G.; Ramadwar, M.; Shrikhande, S. V.; Gupta, S. p38-MAPK/MSK1-Mediated Overexpression of Histone H3 Serine 10 Phosphorylation Defines Distance-Dependent Prognostic Value of Negative Resection Margin in Gastric Cancer. *Clinical Epigenetics* **2016**, *8*, 88.
- (20) Commodaro, A. G.; Bombardieri, C. R.; Peron, J. P. S.; Saito, K. C.; Guedes, P. M.; Hamassaki, D. E.; Belfort, R. N.; Rizzo, L. V.; Belfort, R.; de Camargo, M. M. p38 α MAP Kinase Controls IL-17 Synthesis in Vogt-Koyanagi-Harada Syndrome and Experimental Autoimmune Uveitis. *Invest. Ophthalmol. Vis. Sci.* **2010**, *51*, 3567–3574.
- (21) Kawaguchi, M.; Fujita, J.; Kokubu, F.; Huang, S.-K.; Homma, T.; Matsukura, S.; Adachi, M.; Hizawa, N. IL-17F-Induced IL-11 Release in Bronchial Epithelial Cells via MSK1-CREB pathway. *Am. J. Physiol. Lung Cell. Mol. Physiol.* **2009**, *296*, L804–L810.
- (22) Ota, K.; Kawaguchi, M.; Matsukura, S.; Kurokawa, M.; Kokubu, F.; Fujita, J.; Morishima, Y.; Huang, S.-K.; Ishii, Y.; Satoh, H.; Hizawa, N. Potential Involvement of IL-17F in Asthma. *J. Immunol. Res.* **2014**, *60285–60286*.
- (23) Bamford, M. J.; Bailey, N.; Davies, S.; Dean, D. K.; Francis, L.; Panchal, T. A.; Parr, C. A.; Sehmi, S.; Steadman, J. G.; Takle, A. K.; Townsend, J. T.; Wilson, D. M. (1H-Imidazo[4,5-c]pyridin-2-yl)-1,2,5-oxadiazol-3-ylamine Derivatives: Further Optimisation as Highly Potent and Selective MSK-1-Inhibitors. *Bioorg. Med. Chem. Lett.* **2005**, *15*, 3407–3411.
- (24) Naqvi, S.; Macdonald, A.; McCoy, C. E.; Darragh, J.; Reith, A. D.; Arthur, J. S. C. Characterization of the Cellular Action of the MSK Inhibitor SB-747651A. *Biochem. J.* **2012**, *441*, 347–357.
- (25) Caliper Technol, NanoSyn.
- (26) Miller, R. M.; Paavilainen, V. O.; Krishnan, S.; Serafimova, I. M.; Taunton, J. Electrophilic Fragment-Based Design of Reversible Covalent Kinase Inhibitors. *J. Am. Chem. Soc.* **2013**, *135*, 5298–5301.
- (27) Krishnan, S.; Miller, R. M.; Tian, B.; Mullins, R. D.; Jacobson, M. P.; Taunton, J. Design of Reversible, Cysteine-Targeted Michael Acceptors Guided by Kinetic and Computational Analysis. *J. Am. Chem. Soc.* **2014**, *136*, 12624–12630.
- (28) Control = 1-pyrimidin-4-ylpyrrolo[3,2-c]pyridine. Cascade ERK2-MSK1 pIC₅₀ 5.8. This compound lacks Cl-atoms on the pyrimidine, hence negating any potential covalent reaction.



(29) Le Questel, J.-Y.; Berthelot, M.; Laurence, C. Hydrogen-Bond Properties of Nitriles: A Combined Crystallographic and *ab initio* Theoretical Investigation. *J. Phys. Org. Chem.* **2000**, *13*, 347–358.

(30) KINOMEscan by DiscoverX (Eurofins).

(31) Song, Y.; Bridges, A. J. Selective Inhibitors of Clinically Important Mutants of the EGFR Tyrosine Kinase. PCT patent application WO2017120429, July 13, 2017.

(32) Luo, H.; Zhou, H.; Wang, S.; Wu, Y. Pyridine Aminopyrimidine Derivative, Preparation Method and Use Thereof. PCT patent application WO2016015453, February 4, 2016.